JOURNAL OF Materials CHEMISTRY

A monolayer dispersion study of titania-supported copper oxide

Xiao-Feng Yu,* Nian-Zu Wu, You-Chang Xie and You-Qi Tang

State Key Laboratory for Structural Chemistry of Unstable & Stable Species, Institute of Physical Chemistry, Peking University, Beijing 100871, China.
E-mail: xiaofeng@pubms.pku.edu.cn; Fax: +86-10-62751725; Tel: +86-10-62751491

Received 16th December 1999, Accepted 11th April 2000
Published on the Web 21st June 2000

A monolayer dispersion of copper oxide on the surface of anatase and its effect on the anatase properties have been studied by BET surface area measurements, transmission electron microscopy (TEM), X-ray photoelectron spectroscopy (XPS), temperature-programmed reduction (TPR), and X-ray diffraction (XRD). XPS results give a monolayer dispersion threshold of 5.1 mg CuO (g TiO_2)$^{-1}$. Strong interactions between CuO and anatase can be seen from the TPR results. When the loading of CuO is below its monolayer dispersion threshold, the onset temperature of the anatase–rutile transformation and the transition speed strongly depend on the dispersion of CuO. Crystalline CuO appears when the CuO loading is higher than the monolayer dispersion threshold, but it has little effect on the phase transformation of the samples.

Introduction

Metal oxide–oxide support interactions have attracted much attention because of the wide applications of supported metal oxide systems. It has been well demonstrated that under appropriate conditions many kinds of metal oxides can be dispersed on the surface of the supports. Xie and Tang[1] doped various oxides or salts, such as MoO_3, $CuCl_2$, La_2O_3, and NaCl, on γ-alumina, silica or titania by the impregnation or thermal dispersion methods. They found that monolayer dispersion is a common or even ubiquitous form rather than a rare occurrence. A great many oxides and salts can disperse spontaneously onto the surface of supports to form a monolayer or submonolayer, because in these cases the monolayer is a thermodynamically stable form. Furthermore, there are many unique effects when compounds disperse as monolayers on supports.[2–6]

The study of titanium oxide continues to be interesting because of its applications as a photocatalyst, an opacifier, a white pigment in paints, an ingredient of enamels and glazes as well as its applications in electronic devices.[7–9] Also, titania is an important support widely used in catalysis and has received much attention.[10–12] Synthetic titania crystallizes in two polymorphs: anatase and rutile. Anatase is metastable and transforms exothermally and irreversibly to rutile. Some properties of titania may strongly depend on its polymorphic phase.[13,14] The anatase–rutile transition is strongly influenced by the synthesis method, atmosphere, grain growth and impurities.[15–17] Some additives, such as ZrO_2[18] and Al_2O_3,[19] retard the anatase–rutile transition, whereas others, such as CoO and ZnO,[20] accelerate such a process.

In this paper, we report the monolayer dispersion of CuO on titania. It has strong effects on the reduction behavior of copper oxide in CuO/TiO_2 samples. Also, it is a simple and effective method to influence the anatase–rutile phase transition.

Experimental

The TiO_2 support was impregnated in aqueous solutions containing the required amount of $Cu(NO_3)_2{\cdot}3H_2O$ and the solutions were dried at 373 K with continuous stirring. The impregnated samples were dried at 393 K and calcined at 973 K for 8 h.

The BET surface areas of the samples were measured using a Micromeritics ASAP 2010 instrument with a computer-controlled measurement system. The samples were evacuated at 623 K to a vacuum <4 μm Hg before measurement.

The phase identification was carried out by means of a BD-86 X-ray diffractometer, employing Cu-Kα (Ni filtered) radiation of wavelength 1.54 Å. The accelerating voltage was 40 kV and the anode current was 20 mA. The data were taken in the range of 10–70 degrees (2θ) using a step size of 0.02 degrees where the time for data collection per step was 0.15 s. The anatase–rutile transformation rate, f, was determined by using the following equation[21]

$$f = \frac{1}{1+0.8\times\frac{I_{A(101)}}{I_{R(110)}}}\times 100\% \quad (1)$$

where $I_{A(101)}$ is the integral intensity corresponding to the (101) peak for anatase and $I_{R(110)}$ is the integral intensity corresponding to the (110) peak for rutile. The XRD line broadening was carried out using a Rigaku Rotaflex diffractometer employing Ni-filtered Cu-Kα radiation ($\lambda = 1.54$ Å). The X-ray tube was operated at 40 kV and 120 mA. The DS (divergence slit) was 1 degree, the SS (scattering slit) was 1.2 mm and the RS (reception slit) was 0.4 mm. The crystal size was obtained by using the following equation:

$$D = K\lambda/(B-B_0)\cos\theta \quad (2)$$

where D is the crystal size, θ is the diffraction angle, K is a constant (0.9), B_0 is the FWHM of the diffraction peak when the crystalline peak is very big and has no line broadening, B is the FWHM of the sample.

The XPS spectra were obtained with a VG-ESCALAB 5 spectrometer. An Al-K$\alpha_{1,2}$ X-ray source was used and the anode operated at 9 kV and 18.5 mA. The chamber pressure was kept at 10^{-8} Torr. The pass energy of analyzer was fixed at 100 eV. The XPS peak intensity ratio between an appointed energy level of Cu2p and Ti2p was taken as a measurement of the surface concentration of CuO on TiO_2.

Temperature-programmed reduction (TPR) was carried out at a heating rate of 10 K min^{-1}, and hydrogen consumption was monitored by a thermal conductivity cell. The flow rate of the H_2/Ar mixture (5% H_2 by volume) was 20 mL min^{-1}. The reactor was made of quartz tubing and the sample (150 mg) was mounted on loosely packed quartz wool.

The TEM was performed using a JEM-100 CX Hitachi microscope operating at 100 kV.

DOI: 10.1039/a909893c

Table 1 The BET surface areas of some samples

Sample/mg CuO (g TiO_2)$^{-1}$	Pure anatase	1	3	5.9	15.6	29.2
BET surface area/m^2 g^{-1}	9.6	9.4	8.9	8.6	8.7	7.1

Table 2 The FWHM and crystal size of some samples

Sample/mg CuO (g TiO_2)$^{-1}$	Pure anatase	1	3	5.9	15.6	29.2
$B-B_0$ (FWHM)/degrees	0.111	0.121	0.111	0.108	0.106	0.115
Crystal size (D)/Å	792	727	792	814	829	765

Results and discussion

The BET surface areas of the CuO/TiO_2 samples are shown in Table 1. From the table one can see that there is little change in the surface areas of samples with different amounts of CuO loading. The XRD peak FWHM was measured and the crystal sizes of the samples were calculated by using eqn. (2) (as shown in Table 2). After the CuO was loaded on anatase, the crystal sizes of the samples were not obviously changed. The TEM results also showed the same thing (as shown in Fig. 1). It seems that the loading of CuO has no appreciable effect on the surface morphology of the TiO_2 support from all these results.

Because the content of CuO is very small (the largest value is 29 mg CuO (g TiO_2)$^{-1}$), it is very difficult to determine the amount of crystalline CuO in CuO/TiO_2 by XRD quantitative phase analysis. The CuO/TiO_2 samples were prepared by impregnation. So CuO may disperse on the surface of TiO_2 in some form. X-Ray photoelectron spectroscopy (XPS) is a surface-sensitive technique. Fig. 2 shows the Cu2p and Ti2p spectra of some samples. The XPS peak intensity ratios I_{Cu2p}/I_{Ti2p} as a function of CuO content were determined to identify the state of CuO in CuO/TiO_2, as shown in Fig. 3. The resulting curve can be thought of as being made up of two lines with different slopes, and the amount of CuO at the intersection point of the extrapolated lines is about 5.1 mg CuO (g TiO_2)$^{-1}$. For CuO contents below 5.1 mg CuO (g TiO_2)$^{-1}$, the slope of the I_{Cu2p}/I_{Ti2p} *versus* CuO content curve is steep; when the CuO content is beyond the above value, the slope becomes slight. This means that CuO has dispersed as a monolayer onto the surface of the support TiO_2 when the CuO content is below 5.1 mg (g TiO_2)$^{-1}$, so the I_{Cu2p}/I_{Ti2p} ratio increases quickly with the increase of dispersed CuO. When the CuO content is beyond 5.1 mg (g TiO_2)$^{-1}$, crystalline CuO begins to appear. At this time, the surface of the support is occupied by the dispersed CuO to the maximum extent and the surface area of CuO exposed to the X-ray dose not increase largely. Although I_{Cu2p}/I_{Ti2p} increases with increasing CuO, the degree is much smaller. The point of intersection of the two lines can be regarded as the maximum dispersion capacity, *i.e.* the monolayer dispersion threshold. So it could be concluded that the monolayer dispersion threshold of the CuO/TiO_2 system calcined at 973 K is about 5.1 mg CuO (g TiO_2)$^{-1}$. Furthermore, on the basis of the BET surface area of anatase (9.6 m^2 g^{-1}), we estimate that there are four Cu^{2+} dispersed on every square nm of the anatase surface (4.0 Cu^{2+} (nm^2 TiO_2)$^{-1}$).

The TPR profiles for the samples are shown in Fig. 4. The H_2 consumption per mg CuO, as calculated from the Cu content in the samples and the hydrogen consumption, and the temperatures of the reduction peaks are given in Table 3.

Bulk CuO has only one reduction peak at about 599 K. Most of the CuO in CuO/TiO_2 samples have more than one reduction peak and the reduction temperatures are far lower than bulk CuO. When the content of CuO is 1 mg CuO (g TiO_2)$^{-1}$, the reduction peak is at 537 K. With increasing CuO content, there

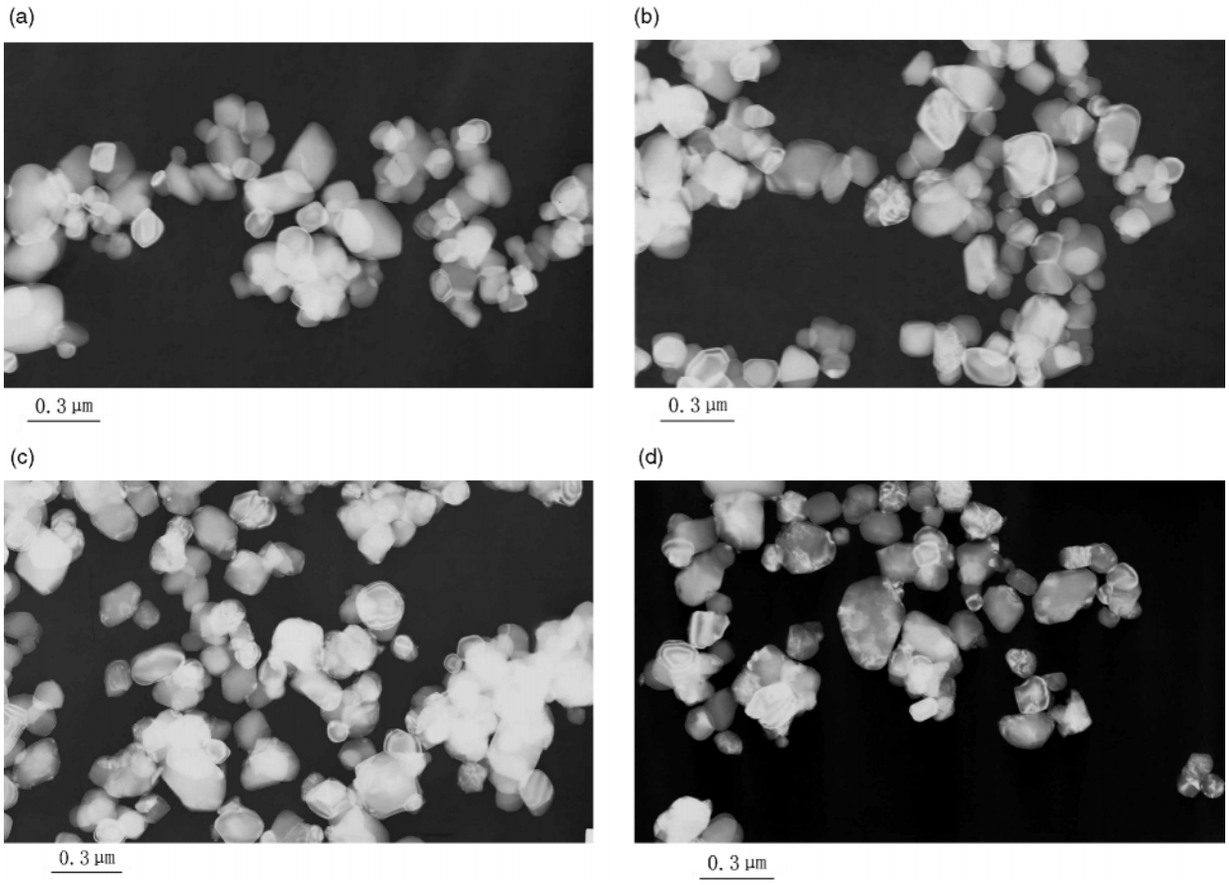

Fig. 1 The TEM images of some samples: (a) pure anatase calcined at 973 K, (b) sample of 1 mg CuO (g TiO_2)$^{-1}$, (c) sample of 7.6 mg CuO (g TiO_2)$^{-1}$, (d) sample of 29.2 mg CuO (g TiO_2)$^{-1}$.

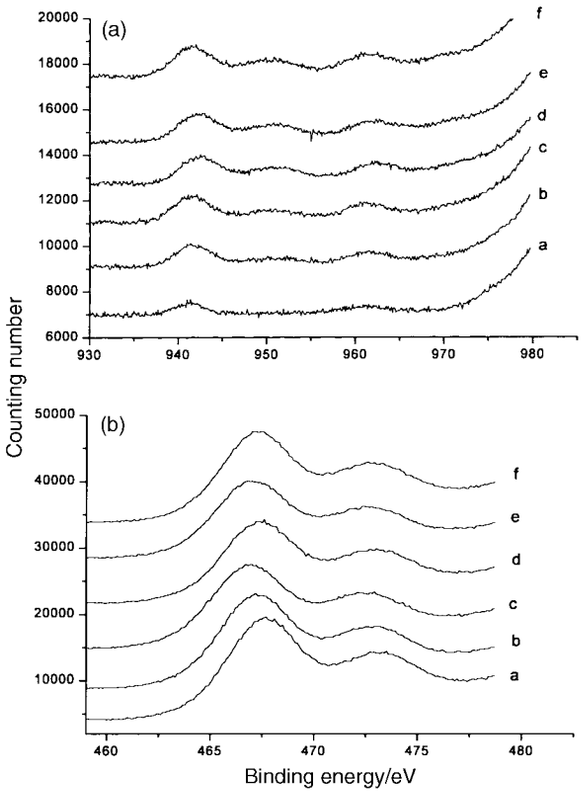

Fig. 2 (a) The Cu2p XPS spectra of some samples. Curves a to f are for samples with CuO contents 1, 3, 4.8, 7.6, 15.6, 29.2 mg CuO (g TiO_2)$^{-1}$. (b) The Ti2p XPS spectra of some samples. Curves a to f are for samples with CuO contents 1, 3, 4.8, 7.6, 15.6, 29.2 mg CuO (g TiO_2)$^{-1}$.

are two peaks and the temperatures of the reduction peaks become lower. It can be concluded that there are strong oxide–support interactions after the CuO is dispersed on the anatase support and the oxide–support interactions have an effect on lowering the reduction temperature of the anatase supported CuO species. The bigger the CuO loading, the stronger the effect. When the CuO loading is about 4.8 mg CuO (g TiO_2)$^{-1}$, another reduction peak at 505 K emerges. From that point, the temperatures of the three peaks remain unchanged and the area of the third peak becomes bigger. It seems reasonable to suggest that the first two peaks correspond to the reduction of the highly dispersed copper oxide and the third corresponds to the crystalline copper oxide. From the reduction behavior, we can conclude that the monolayer dispersion threshold is about 4.8 mg CuO (g TiO_2)$^{-1}$. The reduction behavior agrees with the XPS measurements very well.

Highly dispersed copper oxide has two reduction peaks. This means that there are two different states in the highly dispersed

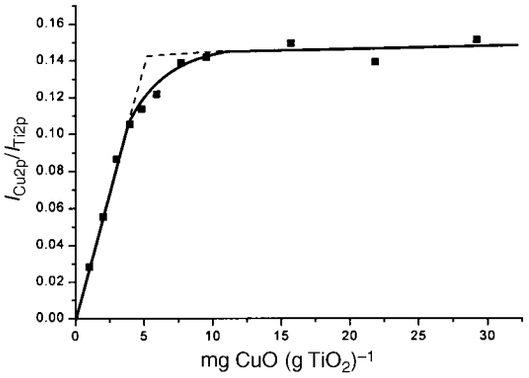

Fig. 3 XPS peak intensity ratio I_{Cu2p}/I_{Ti2p} *versus* the CuO content.

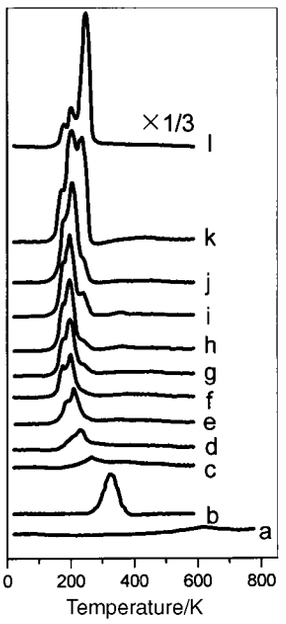

Fig. 4 Temperature-programmed reduction profiles of samples: (a) pure anatase, (b) bulk CuO, (c) 1 mg CuO (g TiO_2)$^{-1}$, (d) 2 mg CuO (g TiO_2)$^{-1}$, (e) 3 mg CuO (g TiO_2)$^{-1}$, (f) 3.9 mg CuO (g TiO_2)$^{-1}$, (g) 4.8 mg CuO (g TiO_2)$^{-1}$, (h) 5.9 mg CuO (g TiO_2)$^{-1}$, (i) 7.6 mg CuO (g TiO_2)$^{-1}$, (j) 9.5 mg CuO (g TiO_2)$^{-1}$, (k)15.6 mg CuO (g TiO_2)$^{-1}$, (l) 29.2 mg CuO (g TiO_2)$^{-1}$. Peak 1 is reduced to 1/3 of its real intensity.

copper oxide. This is interesting and the reason for this is under study.

To study the influence of monolayer dispersed CuO on the anatase–rutile transformation, powder X-ray diffraction was used to determine the phase of titania at different temperatures. Fig. 5 shows the the influence of different contents of dispersed CuO on the anatase–rutile phase transformation. It was found that the CuO additive could noticeably enhance the transformation by reducing the onset transformation temperature. Fig. 5(a) shows the results of heating a pure anatase sample. At 1213 K the titania phase remains anatase. After calcination at 1233 K for 3 h, the diffraction peak of rutile was observed. The anatase was completely converted to rutile after further calcination at 1353 K. However, different behaviour was observed after CuO was monolayer dispersed on titania. Fig. 5(b) shows the results of heating a 1 mg CuO (g TiO_2)$^{-1}$ sample. The anatase phase was maintained at 1153 K, but it began to transform to rutile at 1163 K. The initiation temperature is 60 K lower than that of the pure anatase sample. After further calcination to 1263 K the anatase transformed to rutile completely. Other CuO dispersed samples show similar effects. Fig. 6 shows the percentage of anatase–rutile transformation *versus* temperature for a pure titania sample and for CuO dispersed titania samples with different CuO contents.

The onset transformation temperature was changed markedly. Fig. 7 shows the onset transformation temperature as a function of CuO content. When the CuO content is small, the onset transformation temperature is reduced dramatically; when the CuO content is around the monolayer dispersion threshold, 5.1 mg CuO (g TiO_2)$^{-1}$, the descending speed tends to be slow. When the CuO content exceeds 10 mg CuO (g TiO_2)$^{-1}$, there is no further decrease up to 30 mg CuO (g TiO_2)$^{-1}$.

It can also be seen from Fig. 6 that pure anatase begins its anatase–rutile transformation at 1223 K and ends at 1343 K at the same calcination time. The range of anatase–rutile transformation is 120 K. When the CuO content is 1 mg CuO (g TiO_2)$^{-1}$, the range decreases to 90 K, *i.e.*, from

Table 3 The TPR peak temperatures and H_2 consumption. Letters c to l refer to the curves in Fig. 4

Sample	Temperature/K			H_2 consumption/peak area (mg Cu)$^{-1}$
	1st peak	2nd peak	3rd peak	
bulk CuO			599	21812
c		537		22137
d	458	499		21659
e	452	484		21023
f	442	471		19967
g	444	471	505	22539
h	445	471	509	22532
i	446	471	511	22030
j	450	479	511	23701
k	439	475	512	22858
l	449	475	520	24095

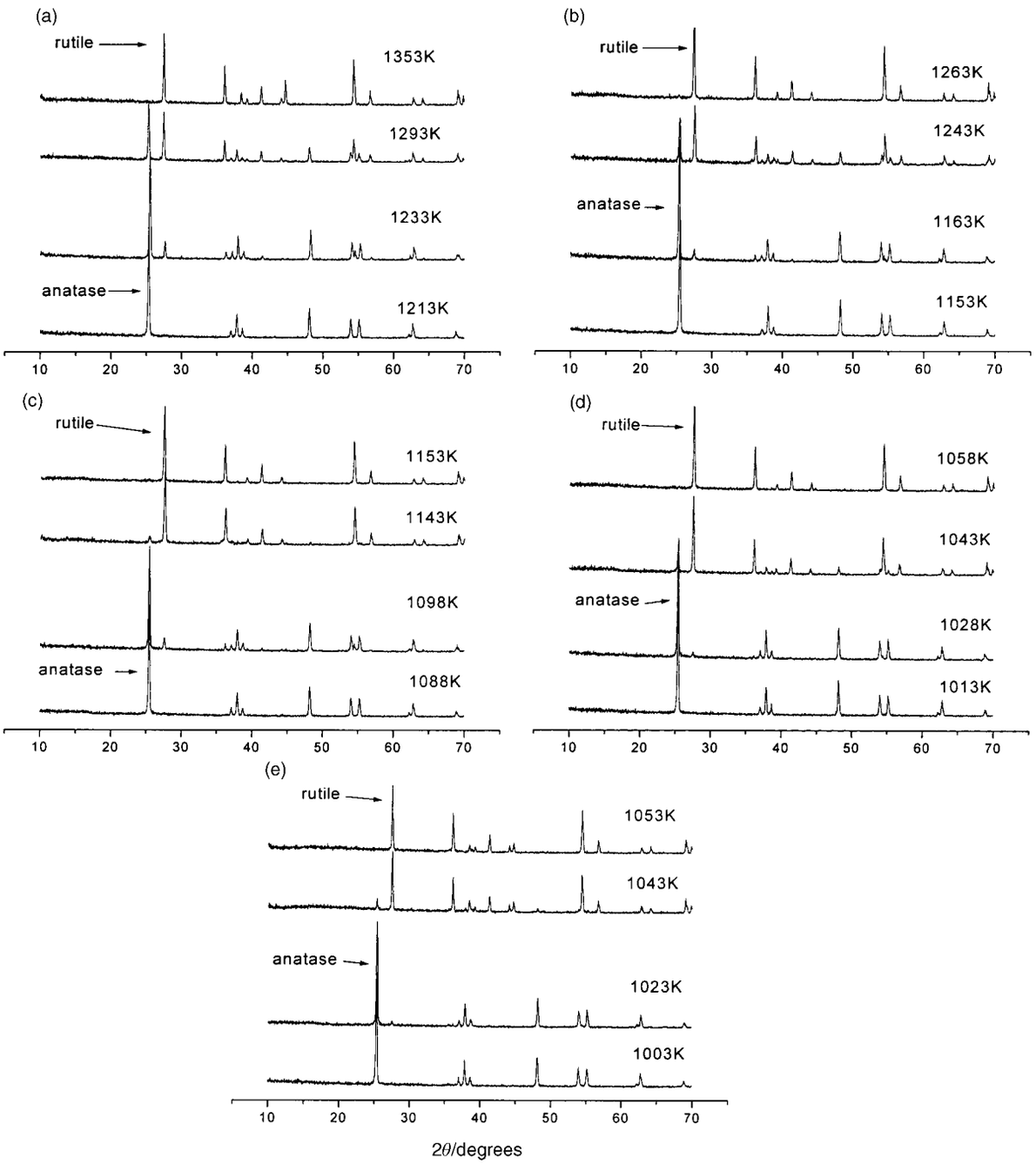

Fig. 5 The XRD profiles, as a function of temperature, of (a) pure anatase; (b) a sample with CuO content 1 mg CuO (g TiO_2); (c) a sample with CuO content 3 mg CuO (g TiO_2); (d) a sample with CuO content 7.6 mg CuO (g TiO_2)$^{-1}$; (e) a sample with CuO content 29.2 mg CuO (g TiO_2)$^{-1}$.

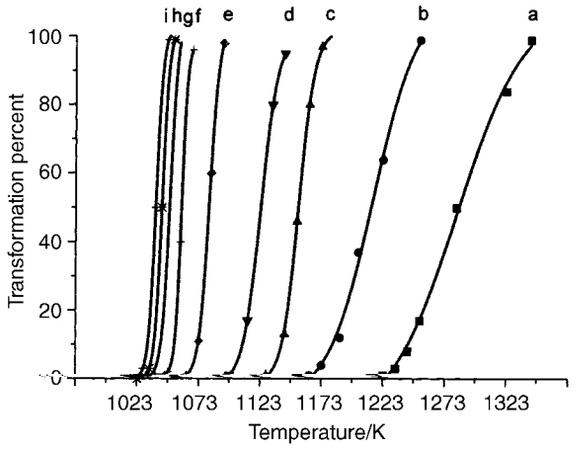

Fig. 6 Percentage of transformation of titania *versus* temperature in air with and without CuO for heating times of 3 hours: (a) pure titania, (b) 1 mg CuO (g TiO_2)$^{-1}$, (c) 2 mg CuO (g TiO_2)$^{-1}$, (d) 3 mg CuO (g TiO_2)$^{-1}$, (e) 3.9 mg CuO (g TiO_2)$^{-1}$, (f) 4.8 mg CuO (g TiO_2)$^{-1}$, (g) 5.9 mg CuO (g TiO_2)$^{-1}$, (h) 7.6 mg CuO (g TiO_2)$^{-1}$; (i) represents 9.5, 15.6, 21.8, 29.2 mg CuO (g TiO_2)$^{-1}$ for which the curves overlap.

1163 to 1253 K. With the increase of CuO content, the range tends to be smaller. However, when the CuO content is near the monolayer dispersion threshold, 5.1 mg CuO (g TiO_2)$^{-1}$, the decrease of range becomes very small. When the amount of CuO is beyond 6 mg CuO (g TiO_2)$^{-1}$, the ranges of temperature remain basically unchanged. Fig. 8 shows the changing tendency of temperature range *versus* CuO content.

In all these cases, no other crystalline phases were detected by XRD (besides CuO, anatase and rutile) in the samples calcined at 1223 K for 8 hours. These results lead to the conclusion that the CuO and the titania support have not reacted to form any new compounds and that the presence of supported copper oxide can promote the anatase–rutile transformation, which should be related to the monolayer dispersion of CuO on anatase. It has been confirmed[22] that the conversion of zirconia from tetragonal to monoclinic starts at the surface of the particles at high temperature and proceeds towards the center of the crystal. It is very likely that in our experiment the same process happened in the anatase–rutile transformation. The highly dispersed CuO might have a strong interaction with the anatase particles as shown by TPR results and the interaction affected the anatase–rutile transformation. The anatase–rutile transformation of CuO-doped anatase happened from the surface much more easily than that of pure anatase. The larger the CuO content, the stronger the accelerating effect was found to be. When the CuO content exceeded the monolayer dispersion threshold, *i.e.*, the maximum dispersion capacity, the available surface of TiO_2 was

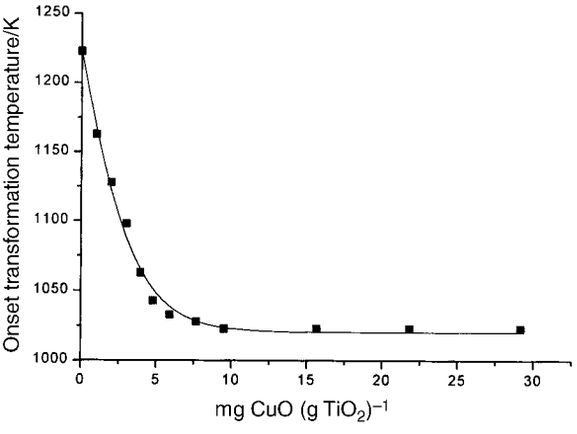

Fig. 7 The onset transformation temperature *versus* CuO loading.

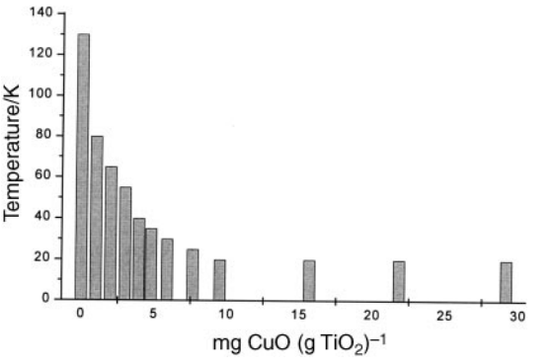

Fig. 8 The temperature range of transformation *versus* CuO loading.

occupied by dispersed CuO, and then crystalline CuO appeared. Because the crystalline CuO could not come into contact with the surface of support, the phase transformation temperature could not be reduced. This behavior suggests an idea that surface monolayer dispersion would affect the anatase–rutile phase transformation effectively and quantitatively. Shannon and Pask[17] found a similar phenomenon and made a suggestion that CuO would completely cover the available surface as a monomolecular layer of the oxide. At the same time, the dispersed CuO could influence the speed of the anatase–rutile transformation. It can be believed that the smaller the temperature range of the anatase–rutile transformation, the higher the transformation speed. When the amount of CuO was small, the monolayer dispersed CuO occupied a small part of the surface of TiO_2. The anatase–rutile transformation could take place only in the region occupied by CuO initially, so the transformation speed was small. With increasing CuO content, the transformation could initially take place over a greater part of the surface, so the transformation speed was higher. However, when the CuO content exceeded the monolayer dispersion threshold, the anatase surface was occupied to the greatest extent, crystalline CuO appeared and could not influence the transformation, so the speed could not be enhanced more and remained unchanged.

Conclusion

In conclusion, CuO can be highly dispersed as a monolayer on anatase by impregnation. The monolayer dispersion threshold of CuO on anatase is 5.1 mg CuO (g TiO_2)$^{-1}$ or 4.0 Cu^{2+} (nm^2 TiO_2)$^{-1}$. There are strong oxide–support interactions after the CuO is dispersed on the anatase support and the oxide–support interactions have an effect on the reduction behavior of the anatase supported CuO species. The reduction temperature of dispersed CuO is changed dramatically and TPR results coincide with those obtained *via* XPS studies. The dispersed CuO can accelerate the anatase–rutile transformation markedly; and the maximum effect is achieved when the amount of CuO is near the monolayer dispersion threshold. At the same time, the transformation speed reaches its highest value at the point near the monolayer dispersion capacity. When the amount of CuO loading is higher than its dispersion capacity, crystalline CuO will appear, which has little effect on the phase transformation of the support as compared to the highly dispersed CuO.

Acknowledgements

This work was supported by a project (No.29733080) from the National Natural Science Foundation of China and a key project in Climbing Program from the Science and Technology Ministry of China.

References

1 Y.-C. Xie and Y.-Q. Tang, *Adv. Catal.*, 1990, **37**, 1.
2 E. C. Alyea, L. J. Lakshmi and Z. Ju, *Langmuir*, 1997, **13**, 5621.
3 T. Ono, M. Anpo and Y. Kubokawa, *J. Phys. Chem.*, 1986, **90**, 4780.
4 Y. Y. Huang, B. Y. Zhao and Y. C. Xie, *Appl. Catal. A: Gen.*, 1998, **171**, 65.
5 K. I. Shimizu, A. Satsuma and T. Hattori, *Appl. Catal. B: Environ.*, 1998, **16**, 319.
6 L. L. Gui, Q. L. Guo, Y. C. Xie and Y. Q. Tang, *Sci. Sin. Ser.B (Engl. Ed.)*, 1984, **27**, 445.
7 G. Dagen and M. Tomkiewiez, *J. Phys. Chem.*, 1993, **97**, 1.
8 R. Debnath and J. Chauduri, *J. Mater. Sci. Lett.*, 1991, **10**, 444.
9 J. Livage, *Mater. Res. Soc. Symp. Proc.*, 1986, **73**, 716.
10 S. J. Tauster, S. C. Fung and R. L. Garten, *J. Am. Chem. Soc.*, 1978, **100**, 170.
11 S. J. Tauster and S. C. Fung, *J. Catal.*, 1978, **55**, 152.
12 A. M. Vannice and R. L. Garten, *J. Catal.*, 1980, **63**, 255.
13 G. Deo, A. M. Turek, I. E. Wachs, T. Machej, J. Haber, N. Das, H. Eckert and A. M. Hirt, *Appl. Catal. A*, 1992, **91**, 27.
14 J. Berry and M. R. Mueller, *Microchem. J.*, 1994, **50**, 28.
15 W. F. Sullivan and J. R. Collman, *J. Inorg. Nucl. Chem.*, 1962, **24**, 645.
16 Y. Iida and S. Ozaki, *J. Am. Ceram. Soc.*, 1961, **44**, 120.
17 R. D. Shannon and J. A. Pask, *J. Am. Ceram. Soc.*, 1965, **48**, 391.
18 J. Yang and J. M. F. Ferreira, *Mater. Res. Bull.*, 1998, **33**, 389.
19 X. Ding, L. Liu, X. Ma, Z. Qi and Y. He, *J. Mater. Sci. Lett.*, 1994, **13**, 462.
20 R. Rodriguez-Talavera, S. Vargas, R. Arroyo-Mutiuo, R. Montiel-Campos and E. Haro-Poniatowski, *J. Mater. Res.*, 1997, **12**, 439.
21 R. A. Spurr and H. Mysers, *Anal. Chem.*, 1957, **29**, 760.
22 J. R. Anderson, in *Structure of Metallic Catalysts*, Academic Press, London, 1975, p. 62.